

Novel one pot synthesis of curcumin quantum dots for non-enzymatic highly sensitive and selective detection of dopamine

B. Iffath, R. Renjithkumar, T. Devasena*

Centre for Nanoscience and Technology, Anna University, Chennai-600025, Tamil Nadu, India

This is the first report on the exploration of the electrocatalytic performance of curcumin quantum dots synthesized by a novel method for nonenzymatic, highly sensitive and selective detection of dopamine. The study was carried out in the presence of high concentrations of its potential neurological interferents having similar oxidation potential to represent real physiological conditions. This proposed novel sensor showed good sensitivity of $14.28 \mu\text{A nM}^{-1} \text{cm}^{-2}$ in the linear range of 0.05 nM to 1 nM, with very low detection limit (0.002 nM) and quantification limit (0.006 nM), which has not been attained by other sensing systems so far.

(Received November 22, 2022; Accepted February 6, 2023)

Keywords: Curcumin, Curcumin quantum dots, Dopamine, Electrochemical sensor

1. Introduction

Dopamine (DA) is an important electrochemically active neurotransmitter produced by the adrenal glands and brain, belonging to the monoamine and catecholamine groups [1]. It plays a vital role in maintaining the functional activities of central nervous, cardiovascular and hormonal systems and also has a significant role in the regulation of cognitive functions such as stress, behavior and attention [2]. DA exists as organic cations in human body, with typical concentration $10\text{--}1000 \text{ nML}^{-1}$ and any fluctuation in this range may lead to several disorders [3,4]. A high DA level indicates cardiotoxicity leading to rapid heart rates, hyper-tension, heart failure, and drug addiction [5]. However, a low DA level may cause stress, Parkinson's disease [6], Schizophrenia [7], Alzheimer's disease [8], depression [9] and attention deficit hyperactivity disorder (ADHD) [1]. Therefore, DA measurement is critical for the early diagnosis of these disorders [10]. Unlike other biological molecules such as glucose, DA is highly redox active and can effectively be measured without the use of other redox couples [11]. However, one critical concern for the detection of DA in blood is its low concentration level (12-16), which is further amplified by the signal interference from other coexisting biomolecules such as glucose, ascorbic acid (AA), and uric acid (UA) whose concentrations are several times greater than DA. Furthermore, AA and UA have similar oxidation potentials and electrochemical properties as that of DA [2]. Additionally, many studies have reported that bare carbon electrodes are unable to clearly distinguish the signals from DA, AA and UA [17]. Most of the DA sensors developed so far are with the detection requirement in the range of 0.3–3 mM, considering DA concentration in human urine [1]. However, there are very few reports on the electrochemical sensing of DA with the detection requirement in the range present in human blood 0–0.25 nM [1]. This necessitates engineering a highly sensitive and selective catalyst to detect the low levels of DA in blood. Most of the reported electrocatalysts for improving the efficiency and selectivity are metal based electrocatalyst which are expensive, and are rarely available in nature [18-20]. Hence, it is necessary to engineer alternative metal-free catalysts as electrochemical sensors that are economically viable, efficient, reproducible and easy to fabricate [21,22].

Curcumin (CM) ($\text{C}_{21}\text{H}_{20}\text{O}_6$) chemically termed as 1,7-bis[4-hydroxy-3-methoxyphenyl]-1,6-heptadiene-3,5-dione, is a natural macrocyclic fluorophore that exhibits a wide range of pharmacological activity, has been proved to be electrochemically active and acts as an electron

* Corresponding author: tdevasenabio@gmail.com

<https://doi.org/10.15251/DJNB.2023.181.183>

donor [23]. Structurally, it is a diferuloylmethane with a heptadiene-dione moiety, is reported to have enhanced the electrochemical signals manifested by various electrochemical studies [24]. The dynamic electrochemical nature of bioactive curcumin could be implicated from its antioxidant activity against the diverse free radicals produced during several physiological processes [22]. Previous studies have reported that CM modified electrodes are capable of offering potentiometric response with good linear ranges for selective analytes belonging to cationic as well as anionic group owing to its the tautomeric keto-enol form [25]. It has also been reported that CM probes could give enhanced performances such as low detection limit, repeatability, reproducibility, high selectivity and high storage stability [26]. The redox behavior of CM could be attributed to the presence of methylene radical at the central 7-carbon chain of CM through the H-shift from the methylene group [27]. Above all, CM is biodegradable and environmentally safe [25].

Studies deploying the electrocatalytic activity of surface functionalized CM in combination with various carbon-based substrates for the electrochemical sensing have been reported earlier [22, 23, 28]. To the best of our knowledge, there is no report on the evaluation of the electrochemical performance of CMQDs towards the electrooxidation of DA. Considering the merits of curcumin in generating electrochemical signals, the present research work was carried out by scaling down the native CM to quantum regime to explore its electrocatalytic performance for developing a highly sensitive and selective detection of DA in the presence of its potential neurological interferents AA and UA with enhanced performance compared to native curcumin-based electrochemical sensors.

2. Experimental

2.1. Materials

The redox mediator curcumin was procured from Sigma Aldrich. Analytes such as dopamine, ascorbic acid, uric acid and glucose were purchased from Himedia. Phosphate buffer saline (PBS) and potassium hexacyanoferrate (K_3FeCN_6) were purchased from SRL, and all other general chemicals for the electrochemical study were of analytical grade. All the solutions and buffers used in this study were prepared using double distilled water.

2.2. Synthesis of CMQD

Photo-oxidative plasma induced irradiation of native curcumin was performed using a focused high energy (100 mJ) beam of infrared wavelength (1064 nm). Distilled water was used as the synthesis medium because it is cheap, safe, exhibits high heat capacity and does not absorb radiation [29]. The beam was then passed through a condensing lens to a spot size of 6 micrometers. The experiment was carried out in room temperature for 15 mins. The generated particles were then characterized for their physical and electrochemical properties.

2.3. Characterization of CMQD

The synthesized curcumin quantum dots were examined for their size, morphology and phase identification using Transmission electron microscopy (TALOSF200S G2), absorption maxima using UV-Visible spectroscopy (T90+ PG INSTRUMENTS), structural integrity using Raman spectroscopy (AGILTRON INC. PEAK SEAKER PRO 532) and the electrochemical studies using electrochemical workstation equipment (BIOLOGIC SAS MODEL SP-150).

3. Results and discussion

3.1. The possible mechanism of formation of CMQDs

As the beam irradiates the native curcumin tablet, photo induced exothermic reactions cause the expansion of the generated plasma plume leading to strong confinement effect. The high temperature and pressure of the plasma heats up the surrounding water, causing it to vaporize, resulting in the formation of liquid-plasma. The chemical reaction between the plume and the

liquid plume causes collapse of the cavitation bubble that releases ablated curcumin particles in water [29-31].

3.2. Physical characterization of CMQDs

The transmission electron microscopy (TEM) images of the different sized CMQDs (Fig.1(a)) shows spherical shaped morphology with an average size of 2.90 nm. The selected area electron diffraction (SAED) pattern depicted in Fig.1(b) reveals a diffuse ring indicating the amorphous nature of CMQDs. The UV-Visible absorption spectra of CMQDs depicted in Fig. 2 exhibits two absorption bands at 240 nm and 370 nm, both in the UV region of electromagnetic spectrum. Fig. 3 represents the Raman spectra of CM and CMQD. The Raman spectra of both native CM (Fig. 3(a)) and CMQD (Fig. 3(b)) were similar, which showed that the chemical composition and major structural parameters do not change when scaled down to quantum regime. Comparison of the Raman spectra of CM and CMQD is presented in Fig. 3(c). Various stretchings and bendings are briefed in Table 1 [32,33].

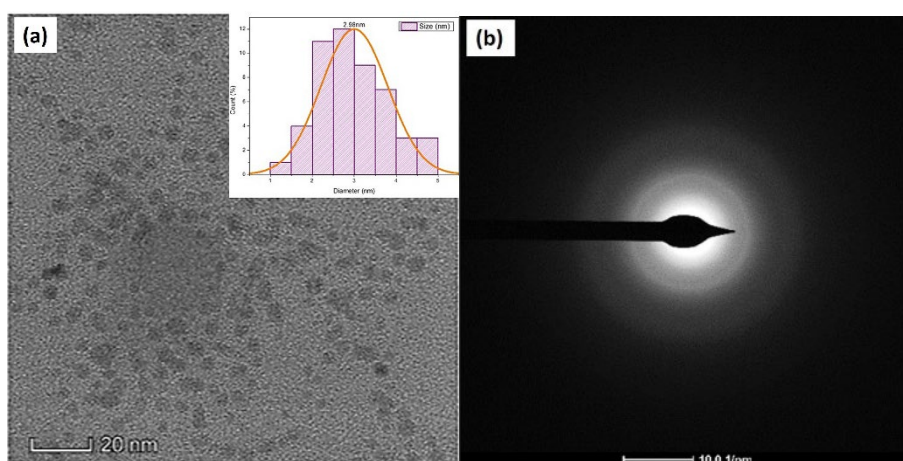


Fig. 1. (a) TEM image of CMQDs. (b) SAED pattern of CMQDs.

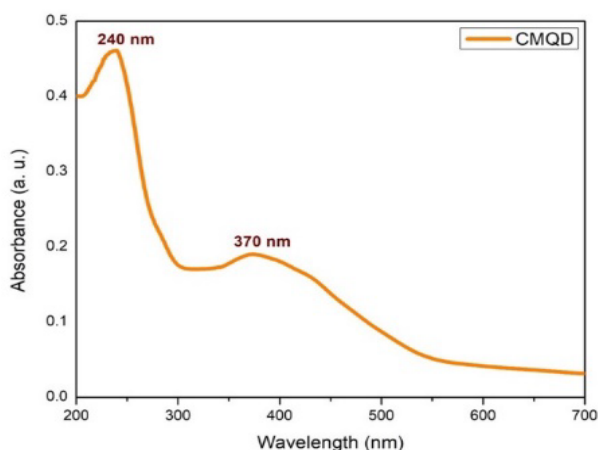


Fig. 2. UV absorption spectrum of CMQDs.

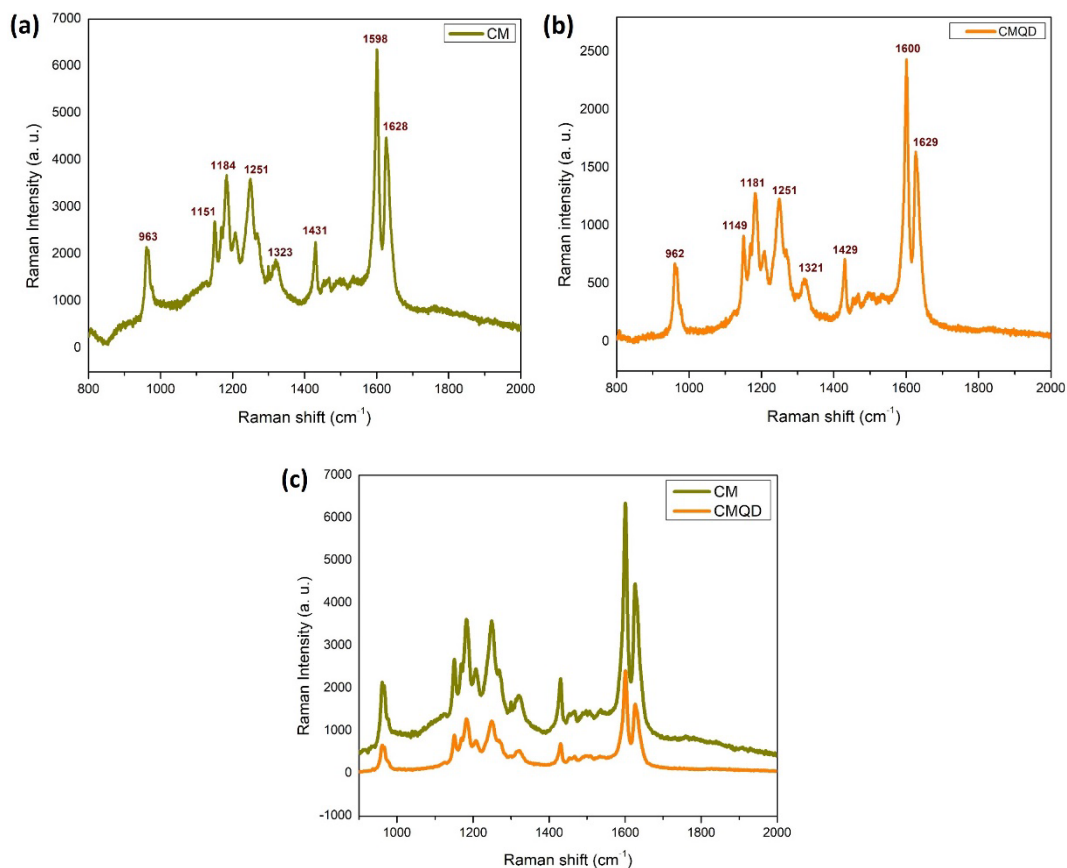


Fig. 3. Raman spectra of (a) CM. (b) CMQD. (c) CM and CMQD.

Table 1. Comparison of the peaks observed in the Raman spectra of CM and CMQDs.

CM peaks (cm ⁻¹)	CMQDs peaks (cm ⁻¹)	Inference
1628	1629	C = O stretching
1598	1600	C-C ring stretching of aromatic ring
1431	1429	C-O stretching of phenol
1324	1321	C-CH stretching
1251	1251	C-O stretching of enol
1184	1181	C-O-C stretching
1151	1149	In plane bending of aromatic CCH and skeletal CCH
963	962	In plane bending of CCH

3.3. Electrochemical characterization of CMQD.

To identify the electrochemical behavior of the synthesized CMQDs electrochemical impedance analysis, cyclic voltammetry analysis and linear sweep voltammetry analysis were performed and compared with native CM modified electrode and bare electrode.

3.3.1. Electrochemical impedance spectroscopy (EIS)

The EIS experiment was performed in 0.1 M PBS solution containing 5 mM K₃Fe(CN)₆ in the frequency range 10 mHz to 100 KHz. Fig. 4 shows changes in the faradic impedance on different electrodes (Bare GCE, CM/GCE and CMQD/GCE). Fig. 4 indicates absence of semicircle in the high frequency region and linear curve in the low frequency regions. The low charge transfer resistance at the electrode-PBS interface could be a possible reason for the absence

of semicircle in the high frequency region of EIS plot. Thus, from Fig. 4, it could be observed that CMQD/GCE shows low resistance compared to CM/GCE and bare GCE, thus indicating better electron transfer in the CMQD/GCE than the other electrodes.

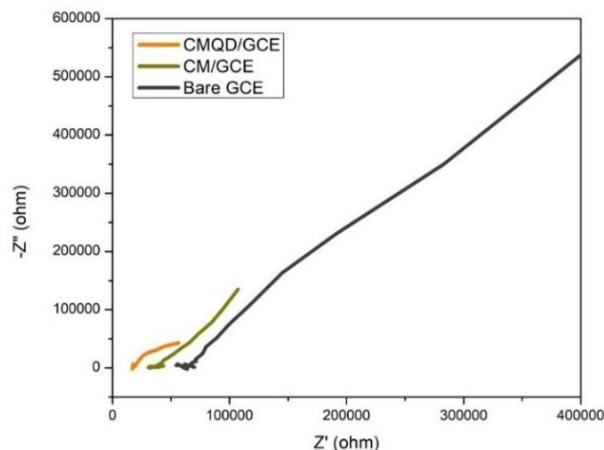


Fig. 4. Electrochemical impedance spectra of bare GCE, CM/GCE and CMQD/GCE.

3.3.2. Cyclic Voltammetry (CV)

The electrochemical responses of the bare/GCE, CM/GCE and CMQD/GCE were studied using CV experiment in 0.1M PBS solution (pH 7), at the scan rate of 50 mVs^{-1} . It could be observed from Fig. 5 that there is no clear oxidation and reduction peak in the bare GCE. While, for CM and CMQD modified electrodes, oxidation and reduction peaks were observed due to the electrocatalytic behavior of CM. Both CM/GCE and CMQD/GCE show anodic (oxidation) peak current (E_{pa}) at 0.6V and cathodic (reduction) peak current (E_{pc}) at -0.2V. But the background current in CMQD/GCE is 1.8 times higher than CM/GCE due more active sites present in the CMQD. As the size of the particle decreases, the surface to volume ratio increases leading to more active sites in the CMQD than the native CM. And also, the quantum confinement effect could be a possible reason for the increase in the electrochemical performance of the CMQD modified electrode compared to the native CM modified electrode. Thus, the prepared CMQD could serve as a good electrode material.

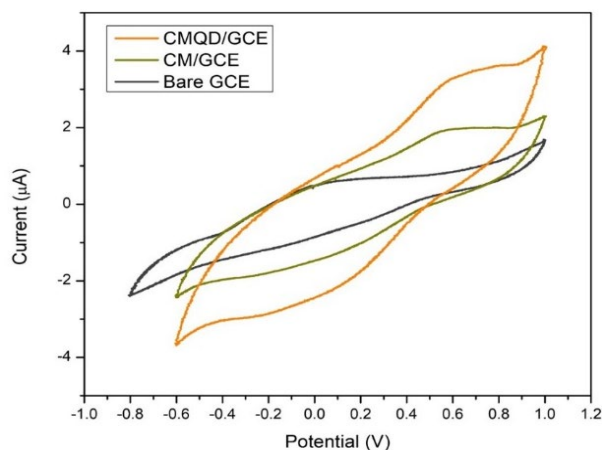


Fig. 5. Cyclic voltammetric response of bare GCE, CM/GCE and CMQD/GCE.

3.4 Analysis of Sensing performance of CMQD/GCE towards DA.

3.4.1. Linear Sweep Voltammetry (LSV)

The electrochemical responses of the modified electrodes (bare/GCE, CM/GCE and CMQD/GCE) towards DA were studied by comparing their linear sweep voltammograms (0 to +1.5 V, 50 mV s⁻¹) in 0.1M PBS (pH 7) containing 1nM DA (Fig. 6). The peak current obtained for CMQD/GCE was 2.3 times higher than CM/GCE indicating its better performance towards DA sensing.

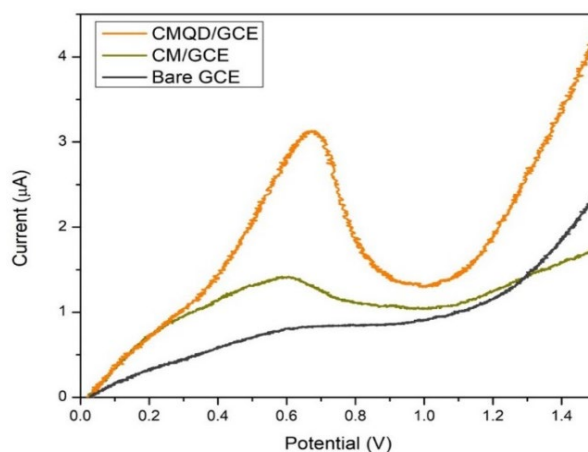


Fig. 6. Linear sweep voltammograms of bare GCE, CM/GCE and CMQD/GCE towards 1nM DA.

3.4.2. Sensitivity of CMQD towards DA

In order to determine the sensing performance of the proposed sensor, the CMQD/GCE was implemented to sense different concentrations of DA (0.05 nM to 1 nM) using LSV technique under optimized conditions (50 mV/s scan rate; potential range: 0 to +1 V). Before adding the analyte, the current responses of the CMQD/GCE were stabilized in 30 ml of 0.1M PBS solution (pH 7). Before each measurement, the electrode was cleaned thoroughly with PBS solution. Fig. 7(a) depicts the current response for every rise in analyte concentration. From Fig. 7(a), it could be observed that, in the absence of DA, the anodic (oxidation) peak appears at 0.6 V, but with the addition of analyte (0.05 nM DA), the peak shifted towards lower potential (0.5 V). As the DA concentration increases from 0.05 nM to 1 nM, a steady increase in current was observed in LSV curve. This study emphasizes that the developed electrode possesses a linear correlation coefficient in low concentration sensing of DA. The corresponding calibration curve, plotted with the obtained peak current (μA) versus the concentration (nM), is illustrated in Fig. 7(b). The linear regression equation was calculated to be $I (\mu\text{A}) = 1.0233x(\text{nM}) + 1.7273$ with $R^2 = 0.99$. The sensitivity for the linear range was calculated from equation 1 and was found to be $14.28 \mu\text{A nM}^{-1} \text{cm}^{-2}$ for 0.05 nM to 1 nM. The detection limit (LOD) and the quantification limit (LOQ) were calculated to be 0.002 nM and 0.006 nM from equation (2) and (3) respectively as per literature evidence [34].

$$\text{Sensitivity} = \text{slope} / \text{electrode area} (0.0707 \text{ cm}^2)$$

$$\text{LOD} = 3.3 \sigma / S$$

$$\text{LOQ} = 10 \sigma / S$$

σ - standard deviation of the y-intercept; S - slope of the calibration curve.

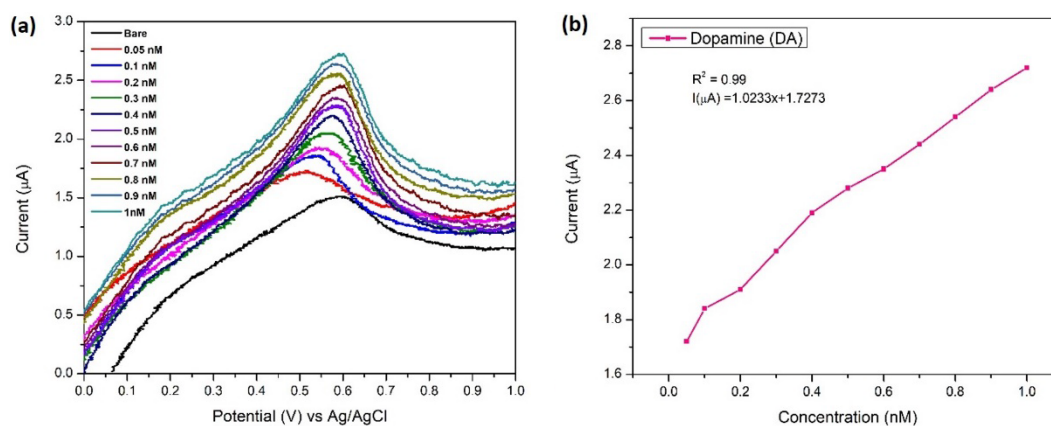


Fig. 7. (a) Linear sweep voltammograms of CMQD/GCE for 0.05 nM to 1 nM concentrations of DA. (b) Corresponding linear plot of anodic peak current versus various concentrations of DA.

To conform the detection limit, the above sensing experiment was repeated three times. The linear range of this study conforms with the detection requirement of DA concentration in human blood (0–0.25 nM) [1]. Detection of such a lower limit of DA is done for the first time through this proposed novel sensor, which has not been attained by other sensing systems. A comparison of curcumin-based electrode materials reported so far and the proposed novel sensor of this study (CMQD/GCE) for DA sensing is tabulated in table 2.

Table 2. Comparison with other publications on DA detection using curcumin based electrochemical sensors.

S. No.	Electrode materials	Method	Linear range (μM)	LOD (μM)	Year	Reference
1.	Oxidized carbon nanotubes with curcumin.	LSV	10 to 170	10	2022	22
2.	Curcumin-functionalized nanocomposite AgNPs/ SDS/ MWCNTs.	CV	12 to 200	0.14	2021	28
3.	Curcumin functionalized gold nanoparticle.	CV	0.4 to 0.56	0.042	2019	23
4.	CMQD	LSV	0.0005 to 0.001	0.002	2022	This work

3.4.3. Possible sensing mechanism

The electron-withdrawing methoxy group of CMQDs probably facilitates the oxidation of DA. Since CMQDs confers a greater number of active sites on its surface, enhanced electrochemical performance could be observed. The enhanced current response could be due to the increase in electron transfer owing to its quantum confinement effect. The mechanism is summarized in Fig. 8.

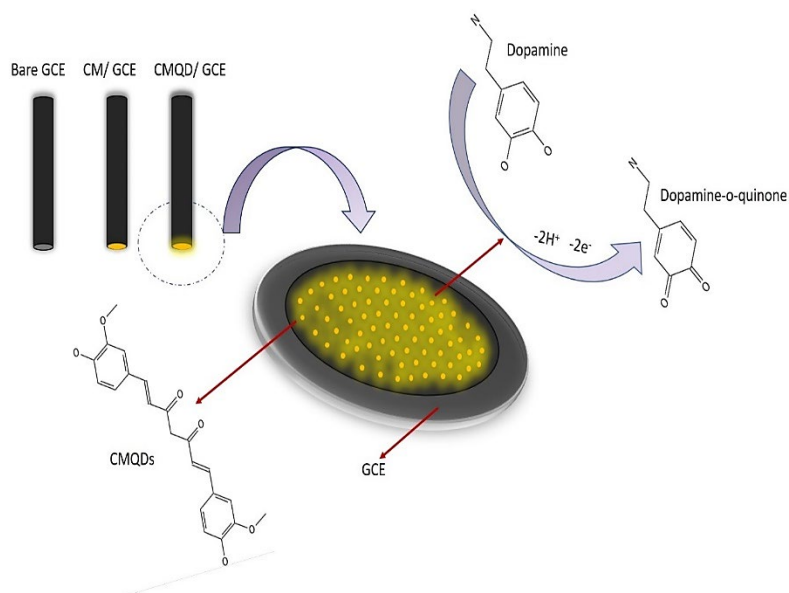


Fig. 8. Pictorial representation of the possible sensing mechanism of the proposed sensor.

3.4.4. Selectivity test

Sensitivity test was carried out using LSV method with 1 nM DA in 0.1M PBS (pH 7), 0-1V potential window and 50 V/s scan rate with three interfering compounds glucose (4.5 mM), UA (5mM) and AA (2.5mM). These concentrations were chosen based on the proportion of each molecule present in the blood serum [1]. From Fig.9, four anodic oxidation peaks could be observed and the highest current response was obtained for DA. The relative closeness of the oxidation peaks could be due to the same oxidation potential of the interfering molecules. However, the difference in the oxidation potential between DA and other interferents is distinct, so it can be stated that CMQD/GCE is highly selective towards the target analyte DA.

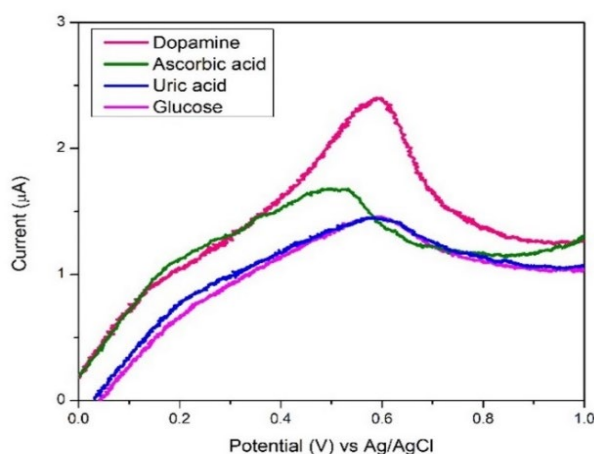


Fig. 9. Selectivity test of CMQD/GCE towards 1 nM DA in the presence of high concentrations of potential interferants (AA, UA and glucose).

3.4.5. Reliability and stability of CMQD sensor

Reliability and stability are the key metrics in order to evaluate the sensing performance of the fabricated electrode. The proposed CMQD/GCE sensor was tested for its reliability by consequently running 12 LSV runs in 1 nM DA. From Fig. 10(a) it could be observed that there was no significant change in the peak current for the first 10 runs. The relative standard deviation

(RSD) for the first 10 runs is 0.4%. After the 10th run, peak current decreased slightly with each run. This could be due to the adsorption of oxidation products on the surface of the electrode, consequently blocking the active sites for new DA molecules. The stability of the CMQD modified electrode was assessed by measuring the current response of the electrode in 1nM DA for 7 alternate days as shown in Fig. 10(b). The same electrode was reused for all the 7 alternate days. After every run, the electrode was stored at room temperature in a vacuum desiccator. For the first 5 alternate days, no significant change in LSV current was observed. After the 5th alternate day, a slight decrease in peak current with an acceptable RSD of 0.6% was observed. This shows the stability of the proposed novel sensor.

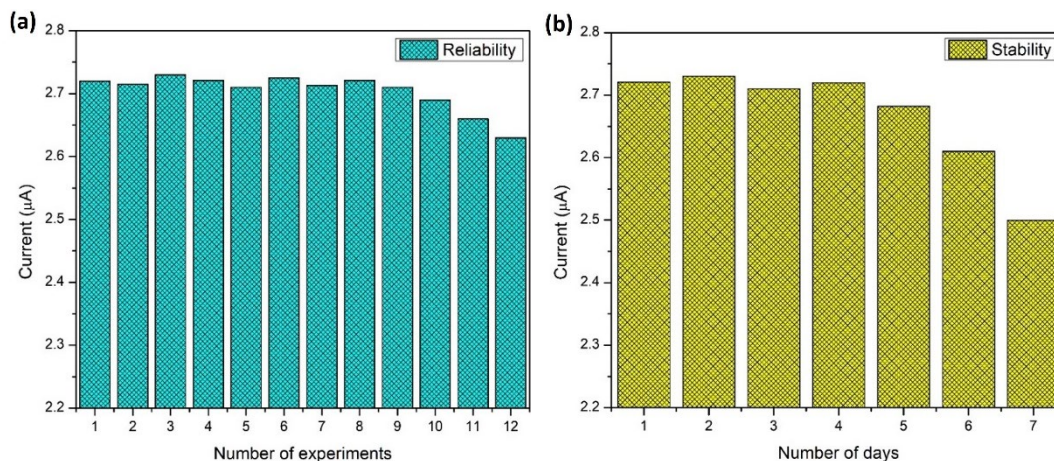


Fig. 10. (a) Reliability of the CMQD sensor. (b) Stability of the CMQD sensor.

4. Conclusion

In this study, we have successfully synthesized novel CMQDs and explored its electrochemical behavior in order to validate its efficacy as electrode material for DA sensing. The redox mediator CMQDs were employed for modifying the surface of GCE for improving the surface area of the electrode and enhancing the sensing performance. A remarkable enhancement in the electrochemical behavior was observed for CMQD/GCE towards DA with good sensitivity of $14.28 \mu\text{A nM}^{-1} \text{cm}^{-2}$ in the linear range of 0.05 nM to 1 nM (that conforms with the detection requirement of DA in blood (0–0.25 nM)), with very low detection limit (0.002 nM) and quantification limit (0.006 nM), even in the presence of high concentrations of interfering molecules, which has not been attained by other sensing systems so far.

Acknowledgements

B. Iffath gratefully acknowledges the AICTE (All India Council for Technical Education), for providing the AICTE Doctoral Fellowship (ADF)-student ID S2022311.

References

- [1] I. Anshori, K. A. Kepakistan, R. L. Nuraviana, A. R. Rona, A. E. Nugroho, R. Siburian, M. Handayani, *Nanocomposites* **8**(1), 155-66 (2022); <https://doi.org/10.1080/20550324.2022.2090050>
- [2] M. Sajid, M. K. Nazal, M. Mansha, A. Alsharaa, S. M. Jillani, C. Basheer, *TrAC Trends in Analytical Chemistry* **76**, 15-29 (2016); <https://doi.org/10.1016/j.trac.2015.09.006>
- [3] T. Masood, M. Asad, S. Riaz, N. Akhtar, A. Hayat, M. A. Shenashen, M. Rahman, *Materials chemistry and physics* **289**, 126451 (2022); <https://doi.org/10.1016/j.matchemphys.2022.126451>

- [4] P. Y. Chen, R. Vittal, P. C. Nien, K. C. Ho, *Biosensors and Bioelectronics* **24**, 3504–3509 (2009); <https://doi.org/10.1016/j.bios.2009.05.003>
- [5] P. J. Feng, Y. L. Chen, L. Zhang, C. G. Qian, X. Z. Xiao, X. Han, Q. D. Shen, *ACS Applied Materials and Interfaces* **10**, 4359 (2018); <https://doi.org/10.1021/acsami.7b12005>
- [6] T. C. Napier, A. Kirby, A. L. Persons, *Progress in Neuro-Psychopharmacology and Biological Psychiatry* **102**, 109942 (2020); <https://doi.org/10.1016/j.pnpbp.2020.109942>
- [7] T. Katthagen, J. Kaminski, A. Heinz, R. Buchert, F. Schlagenhauf, *Schizophrenia bulletin* **48**, 1535-1546 (2020); <https://doi.org/10.1093/schbul/sbaa055>
- [8] X. F. Pan, A. C. Kaminga, S. W. Wen, X. Y. Wu, K. Acheampong, A. Z. Liu, *Front Aging Neuroscience* **11**, 175 (2019); <https://doi.org/10.3389/fnagi.2019.00175>
- [9] A. E. Whitton, J. M. Reinen, M. Slifstein, Y. S. Ang, P. J. McGrath, D. V. Iosifescu, A. Abi-Dargham, D. A. Pizzagalli, F. R. Schneier, *Brain* **143**, 701, (2020); <https://doi.org/10.1093/brain/awaa002>
- [10] X. Liu, J. Liu, *View* **2**(1), 20200102, (2021); <https://doi.org/10.1002/VIW.20200102>
- [11] D. S. Kim, E. S. Kang, S. Baek, S. S. Choo, Y. H. Chung, D. Lee, J. Min, T. H. Kim, *Scientific reports* **8**(1), 1-10 (2018); <https://doi.org/10.1038/s41598-018-32477-0>
- [12] B. Kim, H. S. Song, H. J. Jin, E. J. Park, S. H. Lee, B. Y. Lee, T. H. Park, S. Hong, *Nanotechnology* **24**(28), 285501 (2013); <https://doi.org/10.1088/0957-4484/24/28/285501>
- [13] P. Sivakumar, *Material Research Express* **1**, 045020 (2014); <https://doi.org/10.1088/2053-1591/1/4/045020>
- [14] L. L. Howell, K. A. Cunningham, *Pharmacological Reviews* **67**(1), 176-197 (2015); <https://doi.org/10.1124/pr.114.009514>
- [15] C. Kaya, E. R. Block, A. Sorkin, J. R. Faeder, I. Bahar, *Biophysical journal* **110**(3), 632a (2016); <https://doi.org/10.1016/j.bpj.2015.11.3385>
- [16] M. Meyyappan, *Nano Convergence* **2**, 1-6 (2015); <https://doi.org/10.1186/s40580-015-0049-3>
- [17] A. Manbohi, S. H. Ahmadi, *Sensing and Bio-Sensing Research*, **23**, 100270 (2019); <https://doi.org/10.1016/j.sbsr.2019.100270>
- [18] A. Babaei, A. R. Taheri, *Sensors and Actuators B: Chemical*, **176**, 543–551 (2013); <https://doi.org/10.1016/j.snb.2012.09.021>
- [19] F. R. Caetano, L. B. Felipe, A. J. G. Zarkin, M. F. Bergamini, L. H. Marcolino-junior, *Sensors and Actuators B: Chemical*, **243**, 43–50 (2016); <https://doi.org/10.1016/j.snb.2016.11.096>
- [20] J. R. Ludwig, C. S. Schindler, *Chem.* **2**, 313–316, (2017); <https://doi.org/10.1016/j.chempr.2017.02.014>
- [21] F. Li, B. Ni, Y. Zheng, Y. Huang, G. Li, *Surfaces and Interfaces* **6**, 101375 (2021); <https://doi.org/10.1016/j.surfin.2021.101375>
- [22] S. P. Nayak, V. Prathyusha, J. K. Kumar, *Materials Chemistry and Physics* **287**, 126293 (2022); <https://doi.org/10.1016/j.matchemphys.2022.126293>
- [23] K. K. Kumar, M. Devendiran, R. A. Kalaivani, S. S. Narayanan, *New Journal of Chemistry* **43**, 19003-19013 (2019); <https://doi.org/10.1039/C9NJ04398E>
- [24] B. Devadas, M. Rajkumar, S. M. Chen, *Colloids and Surfaces B: Biointerfaces* **116**, 674–680 (2014); <https://doi.org/10.1016/j.colsurfb.2013.11.002>
- [25] T. Devasena, N. Balasubramanian, N. Muninathan, K. Baskaran, S. T. John, *Bioinorganic Chemistry and Applications* **2022**, 2022; <https://doi.org/10.1155/2022/9248988>
- [26] A. Mejri, A. Mars, H. Elfil, A. H. Hamzaoui, *Microchimica Acta* **185**(12), 529–538 (2018); <https://doi.org/10.1007/s00604-018-3064-3>
- [27] N. S. Jha, S. Mishra, S. K. Jha, A. Surolia, *Electrochimica Acta* **151**, 574–583 (2015); <https://doi.org/10.1016/j.electacta.2014.11.026>
- [28] N. Haghnegahdar, M. Abbasi Tarighat, D. Dastan, *Journal of Materials Science: Materials in Electronics* **32**(5), 5602-5613 (2021); <https://doi.org/10.1007/s10854-021-05282-1>
- [29] M. C. Sportelli, M. Izzi, A. Volpe, M. Clemente, R. A. Picca, A. Ancona, P. M. Lugara, G. Palazzo, N. Cioffi, *Antibiotics*, **7**(3), 67 (2018); <https://doi.org/10.3390/antibiotics7030067>
- [30] R. M. Altuwirqi, *Materials* **15**(17), 5925 (2022); <https://doi.org/10.3390/ma15175925>
- [31] S. Kang, H. Han, K. Lee, K. M. Kim, *ACS omega* **7**(2), 2074-2081 (2022); <https://doi.org/10.1021/acsomega.1c05542>

- [32] A. K. Singh, P. Prakash, R. Singh, N. Nandy, Z. Firdaus, M. Bansal, R. K. Singh, A. Srivastava, J. K. Roy, B. Mishra, R. K. Singh, *Frontiers in microbiology* **8**, 1517 (2017); <https://doi.org/10.3389/fmicb.2017.01517>
- [33] H. Van Nong, L. X. Hung, P. N. Thang, V. D. Chinh, L. Vu, P. T. Dung, V. T. Trung, P. T. Nga, *Springerplus* **5**, 1-9 (2016); <https://doi.org/10.1186/s40064-016-2812-2>
- [34] S. T. K. Fathima, A. A. Banu, T. Devasena, S. Ramaprabhu, *RSC advances* **12**, 19375-19383 (2022); <https://doi.org/10.1039/D2RA01789J>